VDMA
Fluid Power Association

22nd ISC

International Sealing Conference

Stuttgart, Germany
October 01 - 02, 2024

Sealing Technology –
Challenges accepted!

IMA
UNI STUTTGART

ISBN 978-3-8163-0768-6

Fachverband Fluidtechnik im VDMA e. V. Lyoner Str. 18
50628 Frankfurt am Main
Germany

Phone +49 69 6603-1513
E-Mail maximilian.baxmann@vdma.org
Internet www.vdma.org/fluid

A high-pressure radial shaft seal with enhanced wear resistance

Nino Dakov, Martin Franz, Jeff Baehl, Sam Wagoner

High-pressure radial shaft seals are typically used in hydraulic pumps to seal a continuously rotating shaft within a housing bore. When the seal is pressurized, the sealing lip's contact with the shaft increases, which leads to higher wear. At very high pressures, the seal's cross-section can collapse, forcing the garter spring out of its retaining groove. This issue can be mitigated by stiffening the membrane area, though this reduces the seal's ability to accommodate radial movement of the shaft. The current study presents a new approach to stabilize the seal's cross-section. Multiple pads are added on the seal above the membrane area and next to the spring. As a result, a considerably lower laydown is achieved, resulting in improved wear performance during tests. Additionally, the pads help maintain the spring's position. The theoretical considerations are supported by tests conducted under varying pressure and shaft speed conditions, demonstrating the practical benefits of this new seal design.

1 Introduction

Radial shaft seals (RSS), also known as radial oil seals (ROS), are used to seal continuously rotating shafts within housing bores, as depicted in Figure 1. These rubber-to-metal seals typically separate an air side from an oil side. The elastomer-covered metal insert ensures a proper static seal at the outer diameter, adding stability to the sealing profile. The sealing lip features a sharp sealing edge, which is connected to the metal insert by a flexible membrane. The sealing edge is pressed against the shaft and energized by a garter spring [1-2].

The contact force, also referred to as radial force or radial load, between the seal and the shaft results from both a garter spring as well as the elastic deformation of

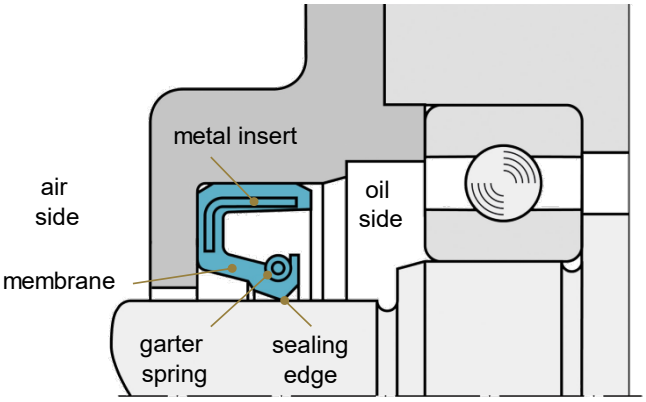

Figure 1: Schematic of a radial shaft seal

the seal due to the overlap with the shaft. The sealing edge is further characterized by an air side contact angle to the shaft that is smaller than the oil side contact angle, creating an asymmetric contact pressure distribution. The asymmetry in contact pressure is essential for reliable dynamic sealing [1].

The membrane adds flexibility to the sealing edge, allowing it to accommodate the misalignment-induced oscillations of the shaft during operation. By design, the RSS is capable of sealing against pressure from the oil side. When the seal is pressurized, both the membrane and the sealing edge are pressed firmly onto the shaft. The pressure activation of the lip ensures leak-tight sealing under high pressure on the oil side. However, increased pressure also enlarges the contact area, leading to higher friction, elevated contact temperatures, and ultimately, accelerated wear of the seal [2].

1.1 High-pressure radial shaft seals

High-pressure radial shaft seals are typically used in gearboxes, hydraulic pumps and motors, speed reducers and robotic applications. To endure the additional load on the lip from pressure activation, these seals feature special lip designs. For high pressure environments, designs are optimized to reduce the laydown of the sealing lip on the shaft typically by either shortening or thickening the membrane, thereby increasing the membrane's stiffness [1], Figure 2. Additionally, the use of a harder elastomer grade can further enhance performance. The metal insert is overmolded with a thicker elastomer layer and reinforced with an axial support, ensuring the spring remains in place even when the sealing lip is strongly deformed.

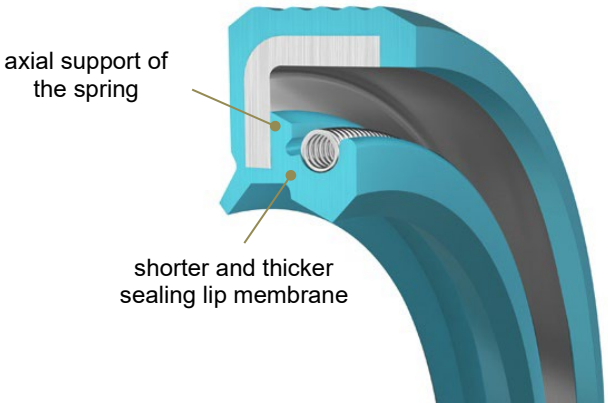

Figure 2: Design aspects of high-pressure radial shaft seals

However, there is an upper limit to how much the membrane area can be stiffened. Some flexibility of the sealing lip is essential for the RSS to compensate for shaft runout. Additionally, as the membrane becomes stiffer, the radial load increases.

Excessive radial load leads to unwarranted friction and wear, potentially causing premature thermal failure of the sealing system.

1.2 Performance criteria

To assess the dynamic properties of a high-pressure RSS, different performance criteria are considered:

- Leak-tightness
- Friction torque and contact temperature
- Wear resistance

Indication as to how well the criteria are met, can be drawn from analytical and numerical calculations. Actual tests are then carried out to measure performance criteria and validate the design.

2 Materials and methods

Finite element analysis (FEA) was used to evaluate the deformation and stress state of the seal. Subsequently, a dynamic test was conducted to validate the design's wear performance, as well as other general factors such as friction torque and contact temperature.

2.1 Simulation approach

A 3D-FEA model is utilized to analyze the deformation and stress state of the seal, focusing on a circumferential segment spanning 60 degrees. The mechanical properties of the 75 ShA fluoroelastomer (FKM) material were characterized using a hyper-elastic material model. The actual 3D geometry of the spring was included in the FEA to study the interaction between the spring and the spring groove. The metal insert was excluded, with nodes contacting the metal fixed in all possible degrees of freedom. The assembly of the seal into the housing, and consequently the effect of the static sealing at the outer diameter, were omitted from the analysis.

The FEA consisted of four analysis steps:

1. Assembling the garter spring into the spring groove.
2. Mounting the radial shaft seal onto the shaft.
3. Increasing the temperature to the fluid's operating temperature of 70 °C, accounting for thermal expansion and softening of the elastomer.
4. Pressurizing the seal to 10 bar.

In the numerical model, the contact stress between the seal and the shaft under higher pressure were examined in detail. The contact stress is crucial for understanding the seal's leak-tightness and wear behavior during operation. Furthermore, the friction torque and contact temperature were estimated using the radial load of the seal and the contact area between the seal and the shaft.

2.2 Test equipment and procedure

Validation tests are performed to assess the performance of the RSS design. The test rig, shown in Figure 3, consists of a shaft positioned inside the test chamber, with a RSS installed at each end. The shaft is supported by two bearings within the chamber. During testing, a continuous oil flow of 1 liter/min simulates real-world conditions akin to a hydraulic pump or motor. The chamber is fully flooded with oil and the oil temperature is kept constant at 60 °C.

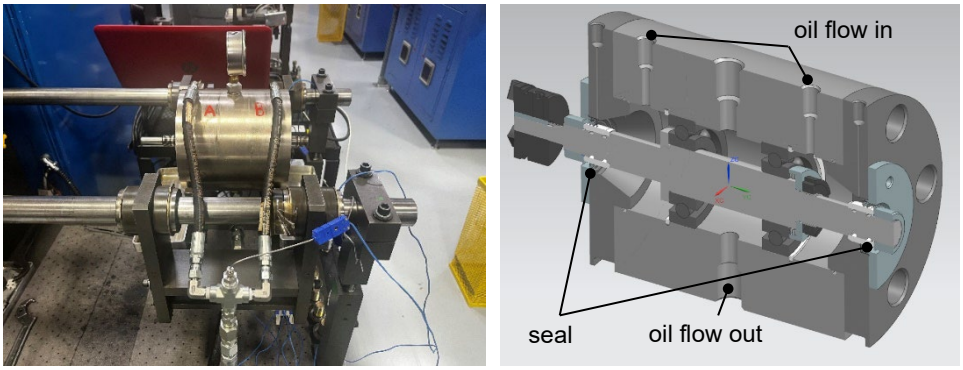

Figure 3: Rotary test rig

The validation tests are carried out at a steady pressure-velocity-value (pv-value) of 10 bar·m/s over a 48-hour period. The following pressure and velocity combinations are examined:

- 3.5 bar x 2.86 m/s
- 5.0 bar x 2.00 m/s

In the test, dynamic leak-tightness is continuously monitored. Any leakage is collected in a beaker and measured. Additionally, friction torque is recorded via a load cell. After the test, the wear of the seal on the shaft is analyzed through light imaging laser profile sensor measurements [3].

The shaft sleeves used are plunge-ground and hardened at ≥ 55 HRC. The surface roughness values, Ra and Rz, range from 0.2 to 0.5 µm and 1.2 to 3.0 µm, respectively. The bearing ratio is maintained between Rmr = 50 to 70 % at a cutting depth of c = 0.25 x Rz.

3 New design for high-pressure radial shaft seals

To prevent the cross-sectionsl collapse under high pressures, pads are incorporated into the radial shaft seal between the garter spring and the shaft, Figure 4. The pads act as an axial stop for the spring. The deformation of the free end of the spring retaining groove is limited locally which results in stabilizing the sealing lip at higher pressure. The example in Figure 4 features a radial shaft seal measuring 28 x 40 x 6 mm with a total of six equally spaced pads along the circumference.

From a manufacturing feasibility standpoint, these pad features are a highly cost-effective performance enhancement, as they can be easily integrated into the tooling process and produced using standard manufacturing techniques.

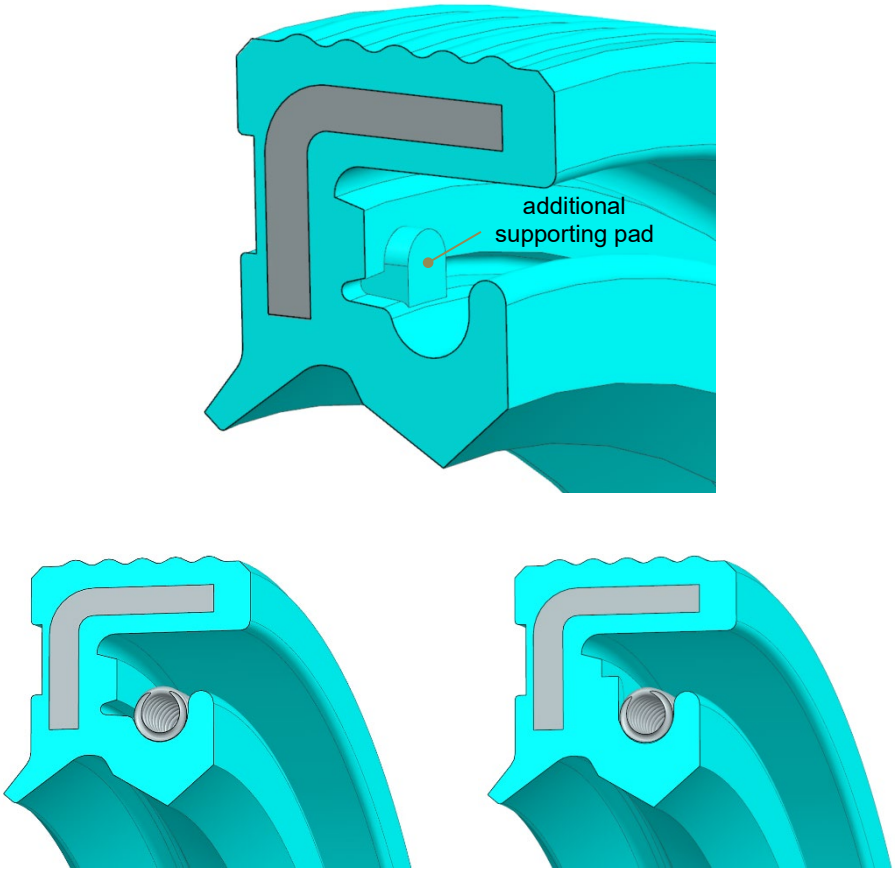

Figure 4: Radial shaft seal design for a pv-value of 10 bar·m/s of size 28 x 40 x 6 mm with six supporting pads (top), section view outside pad (bottom left) and at/near pad (bottom right)

4 Results and discussion

The presented design was analyzed numerically and validated experimentally. The results are summarized and discussed in the following two sections.

4.1 FEA results

The focus of the FEA is on the deformation of the seal under high pressure. The complex interaction between the spring, groove and pad is illustrated using a detailed 3D model of the actual spring in its groove. Figure 5 shows the effect of the pad on the deformation of the seal's cross-section at an overpressure of 10 bar. At the pad's location, the cross-section tilts 27 degrees relative to the radial direction, while outside the pad area, the tilting increases to 34 degrees which is 25 % greater. At the pad, the garter spring provides additional support, acting like a stiff inlay, which stabilizes the lip and reduces deformation at higher pressures. Consequently, the pad locally reduces the laydown of the sealing lip on the shaft.

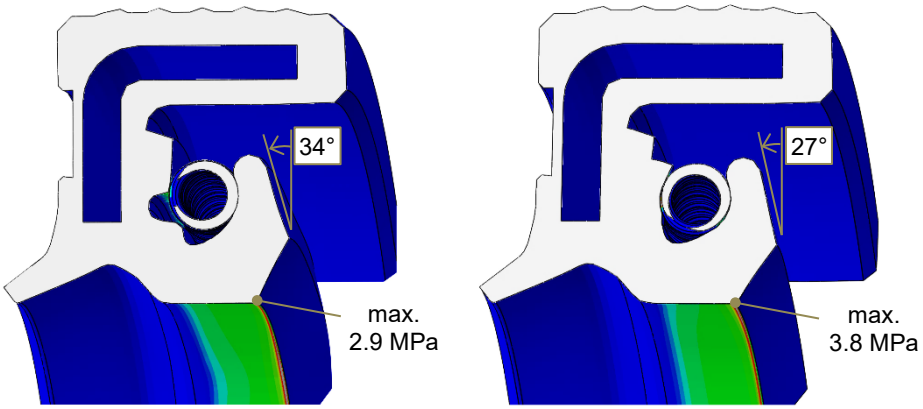

Figure 5: Seal at 10 bar pressure, cross-section at a position without pad (left) and at position of pad (right)

The question arises regarding the effect of the pad at different pressure levels. Figure 6 shows polar plots of the contact band width along the circumference at different pressure values. Starting at 3.5 bar, an undulation of the contact band is visible. The maximum contact width aligns with that of a seal design without supporting pads. At the pad locations, the contact width is reduced, forming a daisy pattern along the seal's circumference. The greatest reduction in contact band width, approximately 15%, occurs at 3.5 and 5 bar. At 7.5 bar, the contact width reduction decreases to about 9 %. Thus, for the given pad design, the optimal reduction in contact area is achieved between 3.5 and 5 bar. Moreover, the pad design can be modified to better achieve a lower contact area within a specific pressure range.

The reduced contact width leads to a lower friction torque and less wear on the seal. Additionally, the undulation in the sealing contact can enhance lubrication underneath the sealing lip, prolonging the lifetime of the seal. Up to an overpressure of approximately 5 bar, the undulation amplitude is proportional to the pressure level, indicating a self-intensifying effect. Above 5 bar, the positive effect stabilizes at an absolute contact band width reduction of about 0.15 mm.

Another aspect that favors improved lubrication is the variation in the maximum contact pressure along the circumference. Figure 5 shows that the contact stress between two pads is 2.9 MPa. At the pad location, the maximum contact stress increases to 3.8 MPa, representing a 30 % increase at the investigated pressure level of 10 bar. This means the contact band width is minimal at the pad, while the contact stress is maximal. These 3D contact area and pressure distributions are deemed favorable for forming a stable lubrication film between the seal and the shaft.

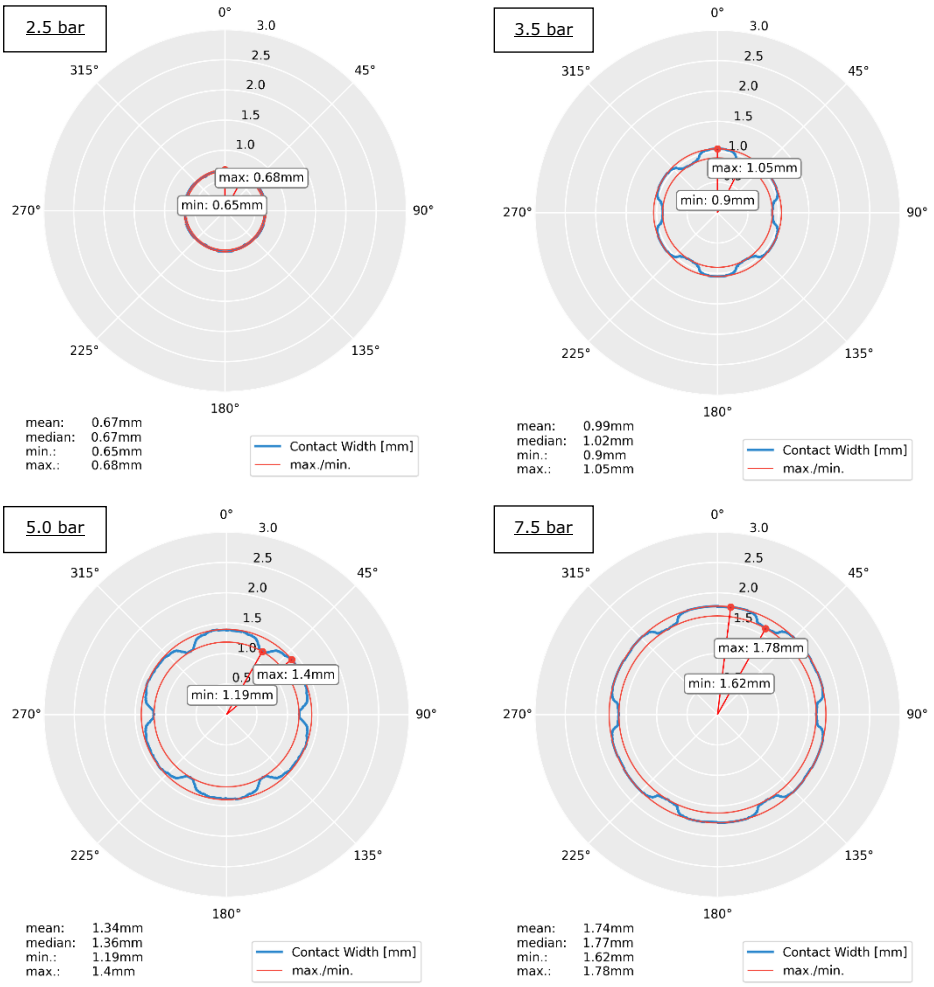

Figure 6: FEA contact band width along circumference at different pressure levels

4.2 Test results

The new seal design concept underwent testing as outlined in Section 2.2, using a standard high-pressure RSS design without supporting pads as a benchmark. All tests were completed without any leakage. The wear results for both pressure and velocity combinations are shown in Figures 7 and 8.

Figures 7 a-b) and 8 a-b) depict light images of the wear tracks in the seals' running areas. Except for the new seal design at 3.5 bar x 2.86 m/s in Figure 7 a), all seals exhibit circumferential grooves and a wear band width (WBW) ranging from 1 to 1.6 mm. The benchmark seals show a significantly wider WBW compared to the padded seals. Furthermore, it can be inferred that at the same pv-value, higher pressure results in a broader WBW. However, visual analysis reveals that the WBW of the new seal design varies along the circumference, making precise quantitative comparison impossible based on a single-spot WBW measurements for each seal.

For a more detailed analysis, the wear track was measured off-shaft over 360° using laser profilometry [2]. A total of 10,000 profiles were recorded along the circumference and assembled into a pseudo 3D plot of the seal's surface, as shown in Figures 7 c-d) and 8 c-d). The left and right borders of the running area, highlighted in green, were identified using a lower and upper limit for the gradient of the profiles in axial direction. From these profiles, it is evident that, in the addition to a greater width, the benchmark seal has a considerably higher maximum depth in the wear track. The circumferential grooves in the benchmark seals' wear track are also visible in the 3D pseudo-topography, indicating more severe damage compared to the padded design.

The WBW was evaluated as the distance between the left and right ends of the wear track, as shown in Figures 7 c-d) and 8 c-d). Quantitative WBW comparisons are displayed as polar plots in Figures 7 e-f) and 8 e-f). Both at 3.5 bar x 2.86 m/s and 5 bar x 2 m/s, the padded seal design exhibits a regular daisy pattern in the WBW. Consistent with the FEA results, the minimum WBW aligns with the location of the pad. At 3.5 bar x 2.86 m/s, the average WBW of the new design is 1.22 mm, which is 20 % less than the benchmark seal's mean width of the wear track of 1.52 mm. At 5 bar x 2 m/s, the average reduction in the wear band due to the stabilizing effect of the pads is 16 %, a similarly substantial decrease.

The reduced contact area of the padded design directly impacts the maximal frictional power loss and contact overtemperature, shown in Figure 9. Contact overtemperature refers to the difference between the contact area's temperature, measured using thermography imaging, and the oil sump temperature in the test. Both seal designs exhibit higher fictional power loss and contact temperature at 3.5 bar and 2.86 m/s compared to 5 bar and 2 m/s. In terms of maximal frictional power loss, a 13 % reduction is achieved at 3.5 bar and 2.86 m/s. Regarding maximal overtemperature, both tests show a significant reduction with the padded design compared to the benchmark. At 3.5 bar and 2.86 m/s, the padded design's contact area

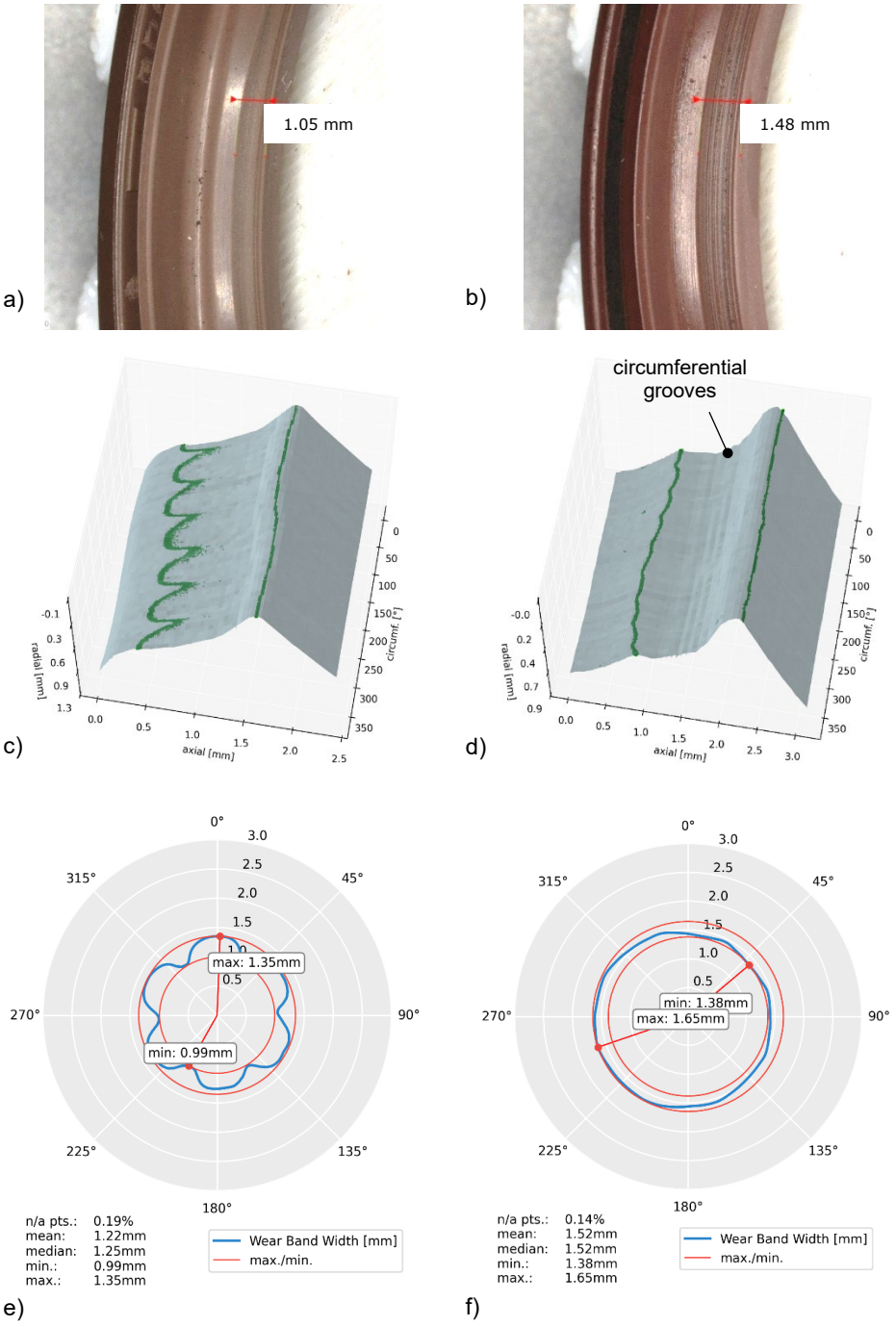

Figure 7: 3.5 bar x 2.86 m/s test, padded design (left) vs benchmark (right): a-b) light image of wear area; c-d) 360° of laser profile measurements; e-f) wear band width

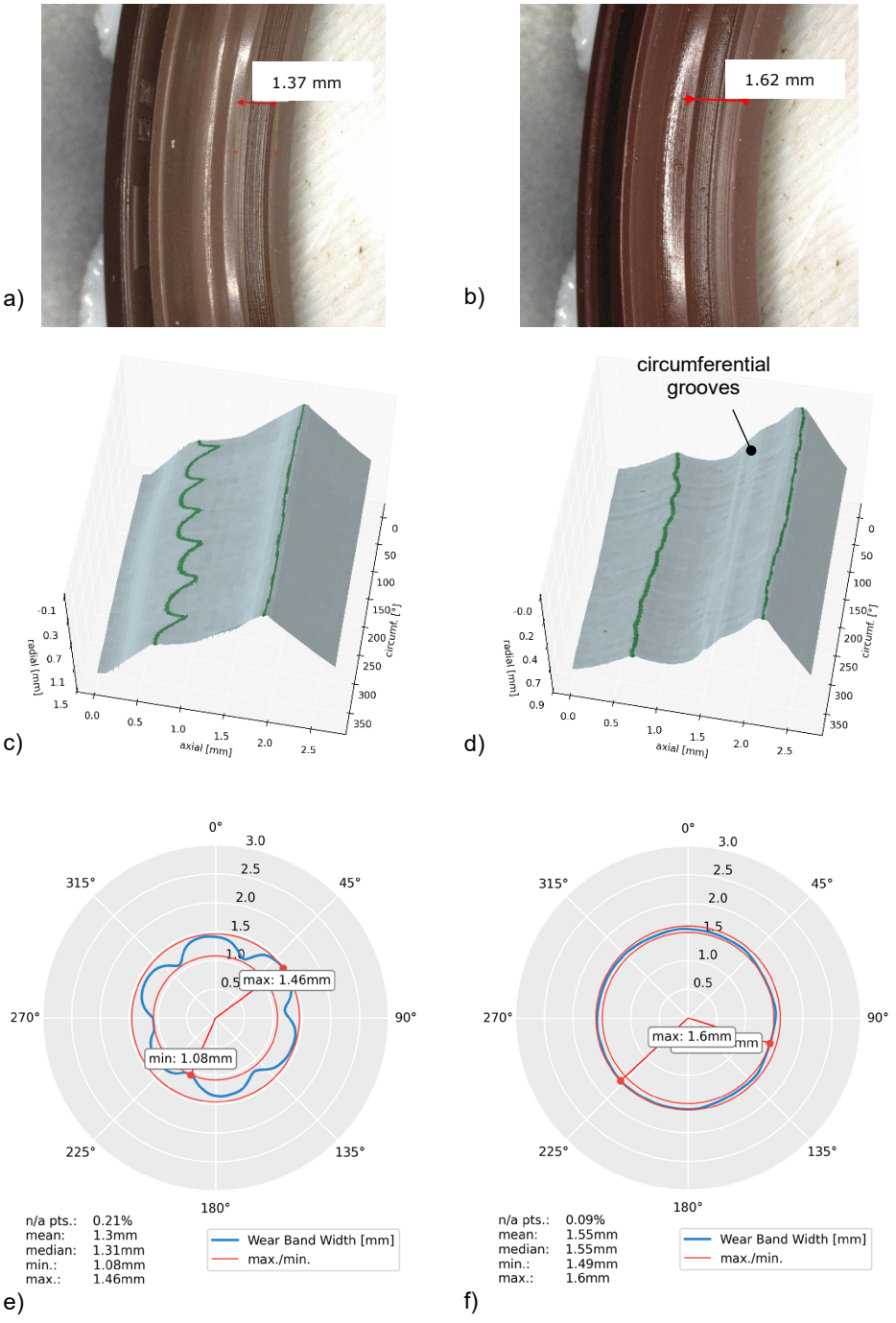

Figure 8: 5 bar x 2 m/s test, padded design (left) vs benchmark (right): a-b) light image of wear area; c-d) 360° of laser profile measurements; e-f) wear band width

is 7 K cooler, while at 5 bar and 2 m/s, the pads provide an advantage of approximately 3 K. Notably, in accordance with the Arrhenius equation [4-5] a 10 K reduction in the temperature can substantially increase service life by nearly halving the speed at which aging effects, such as compression set, occur in the elastomer material.

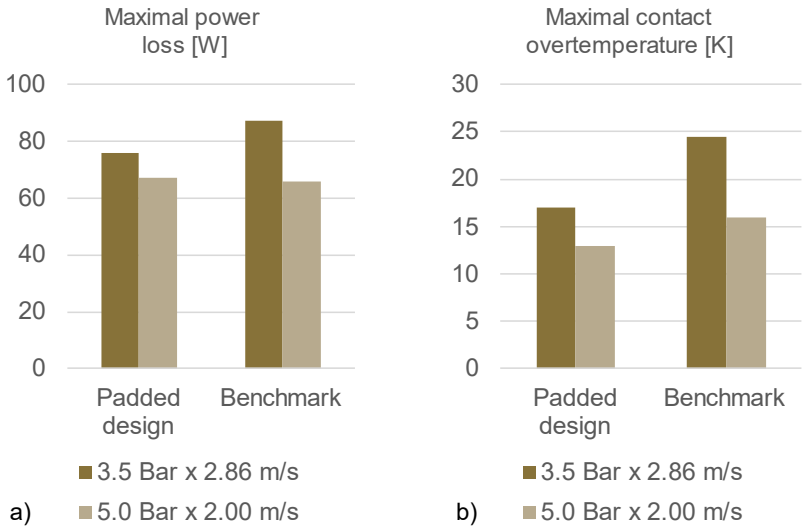

Figure 9: Summary of the measured a) maximal power loss and b) maximal contact overtemperature

5 Summary and conclusion

High-pressure radial shaft seals are essential for various applications, including gearboxes, hydraulic pumps and motors, speed reducers and robotics. To withstand high pressure, these specialized radial shaft seals feature a shorter and thicker sealing lip membrane. In this study, we introduced a new design for a 10 bar·m/s radial shaft seal, incorporating additional pads along the seal's circumference. Under high pressure, the pads stabilize the cross-section by minimizing the laydown of the sealing lip.

A detailed 3D FEA model was used to thoroughly analyze the new design. The results indicated a significant decrease in the contact width at the pad locations for a pressure range from 3.5 to 5 bar. Performance benchmarks were conducted at 3.5 bar x 2.86 m/s and 5 bar x 2 m/s, comparing the padded seal design to a conventional high-pressure seal. The innovative padded design demonstrated considerably improved wear performance, exhibiting a distinct daisy-shaped wear bandwidth pattern consistent with the contact width pattern predicted by FEA.

Moreover, the reduced wear of the new design concept led to lower friction power loss and a decrease in maximal contact temperature during testing. These findings

highlight the overall performance enhancement achieved through the innovative pad feature.

6 References

[1] Müller, H. K., Nau., B. S.: *Fluid sealing technology*, Marcel Dekker, New York, 1998, ISBN 978-0-8247-9969-4.

[2] Horve, L.: *Shaft seals for dynamic applications*. CRC Press, 1996. ISBN 978-0-8247-9716-4.

[3] Baumann, M., & Bauer, F. *Moderne visuelle Untersuchungsmethoden für die Verschleißanalyse am Beispiel Radial-Wellendichtring*, 20th International Sealing Conference 2018, Stuttgart, Germany, 2018.

[4] Gillen, K. T., Bernstein, R., Celina, M.: *Challenges of accelerated aging techniques for elastomer lifetime predictions.* In: *Rubber Chemistry and Technology*, *88*(1), 1-27, 2015.

[5] Wehmann, C., Kulkarni, A., Durn, F., Gulcur, M.: *Modeling the compression set of elastomers to predict the lifetime of sealing systems by finite element analysis*, 21st International Sealing Conference 2022, Stuttgart, Germany, 2022.

7 Authors

Trelleborg Sealing Solutions Germany

Schockenriedstr. 1, 70565 Stuttgart, Germany:

Dr. Nino Dakov

ORCID 0000-0002-0989-9943, nino.dakov@trelleborg.com

Martin Franz

ORCID 0009-0008-0457-9116, martin.franz@trelleborg.com

Trelleborg Sealing Solutions Americas

2531 Bremer Rd, Fort Wayne, IN 46803, USA:

Jeff Baehl

ORCID 0009-0003-6939-1943, jeff.baehl@trelleborg.com

Sam Wagoner

ORCID 0009-0001-5957-0265, sam.wagoner@trelleborg.com

https://doi.org/10.61319/HHAECYDA